Available online at www.sciencedirect.com
SCIENCE DIRECT®
Journal of Sound and Vibration 286 (2005) 963–980
JOURNAL OF SOUND AND VIBRATION
www.elsevier.com/locate/jsvi

Approximate analysis method for interstorey shear forces in structures with active variable stiffness systems

Bo Wu*, Fen-tao Liu, De-min Wei

Department of Civil Engineering, South China University of Technology, Guangzhou 510640, PR China

Received 28 January 2004; received in revised form 12 August 2004; accepted 25 October 2004
Available online 5 January 2005

Abstract

It has been demonstrated that active variable stiffness (AVS) systems may be effective for response control of building structures subjected to earthquake excitations. Because the performance of structures with AVS systems exhibits strong nonlinearity, the classical dynamic analysis method for linear structures, such as the mode-superposition method, is not applicable to structures with AVS systems. In this paper, an approximate analysis method is proposed for the maximum interstorey shear forces in structures with AVS systems. Firstly, a new equivalent relationship between single-degree-of-freedom (sdof) structures with AVS systems and so-called fictitious linear structures is established. Then, the new equivalent relationship is used to revise the approximate-mode-superposition (AMS) approach for multi-degree-of-freedom (mdof) structures with AVS systems, which was previously suggested by the authors. Subsequently, extensive numerical studies are conducted using the revised AMS approach for building structures equipped with AVS systems and subjected to different types of artificial earthquake excitations. Based on the simulation results, an approximate analysis method is proposed for the maximum interstorey shear forces in structures with AVS systems. The maximum interstorey shear forces in example structures subjected to actual earthquake excitations are obtained using the proposed method, and the results are compared with those obtained using the time-history analysis method. It is shown that the results estimated using the proposed method generally agree well with those obtained using the time-history analysis method.

*Corresponding author. Tel.: +86 2087114274; fax: +86 20 87114274.
E-mail address: bowu@scut.edu.cn (B. Wu).

0022-460X/$ - see front matter © 2004 Elsevier Ltd. All rights reserved.
doi:10.1016/j.jsv.2004.10.032

1. Introduction

It has been demonstrated that active variable stiffness (AVS) systems, introduced originally by Kobori at the end of the 1980s, may be effective for response control of building structures subjected to earthquake excitations. Owing to the advantage of no demands for extensive power and energy, the AVS systems have received considerable attention in recent years. Extensive efforts have been devoted to the theoretical and practical development of the AVS systems. Different kinds of control algorithms for the AVS systems have been well investigated by many researchers [1–9]. The effect of the AVS systems on the reduction of seismic responses of high-rise building structures has been demonstrated in papers [10–12]. Such systems have also been tested experimentally and installed on a full-scale test building in Japan [3,13–17]. In the 1990s, the control effectiveness of the AVS systems was verified through a number of observation records [4,18], and some valuable experience concerning the maintenance of the systems was accumulated [5].

The AVS systems consist of stand-by bracings attached to selected storey units of building structures, and the locking and unlocking devices. During an earthquake ground motion, some of the bracings may be locked at a particular time instant, leading to an increase in the stiffness of the corresponding storey units. The locking and unlocking of different bracings at each time instant are regulated by a control algorithm to reduce the structural seismic responses. One of the control algorithms proposed by Kobori and Kamagata is based on the engineering insight as follows. Since the locking of bracing increases the stiffness restoring force, the stand-by bracing should be locked if the interstorey drift, $x(t)$, and its velocity, $\dot{x}(t)$, are both positive or both negative (i.e., $x(t)\dot{x}(t)>0$). On the other hand, if $x(t)$ and $\dot{x}(t)$ are in the opposite direction (i.e., $x(t)\dot{x}(t)<0$), then the stand-by bracing should be unlocked. Such a control algorithm is adopted in this study because of its explicit engineering insight, simple expression form and effectiveness in response control.

The dynamics of structures with AVS systems are highly nonlinear. Therefore, the classical dynamic analysis method for linear structures, such as the mode-superposition method, is not applicable to building structures with AVS systems. At present, the seismic analysis of structures equipped with AVS systems is always conducted using the time-history analysis method, which is obviously inconvenient to be applied in engineering practice. In paper [19], an equivalent relationship between single-degree-of-freedom (sdof) structures with AVS systems and so-called fictitious linear structures was firstly proposed by the authors, and then an approximate-mode-superposition (AMS) approach for multi-degree-of-freedom (mdof) structures with AVS systems was suggested. Finally an approximate analysis method for displacement responses of structures with AVS systems was developed. It has been proven that the approximate analysis method is effective in estimating the maximum relative displacements and the maximum interstorey drifts of structures with AVS systems. In this paper, a new equivalent relationship between sdof structures with AVS systems and so-called fictitious linear structures, which is different from that previously proposed by the authors, is established firstly, and then the new equivalent relationship is used to revise the AMS approach suggested in paper [19]. Subsequently, extensive numerical studies are conducted using the revised AMS approach for 5-, 8- and 12-storey building structures equipped with AVS systems and subjected to different types of artificial earthquake excitations. Based on the simulation results, an approximate analysis method is presented for the maximum interstorey shear forces in structures with AVS systems. The accuracy and efficiency of the proposed method

are investigated through extensive numerical simulations. It is shown that the maximum interstorey shear forces estimated using the proposed method are generally in good agreement with those obtained using the time-history analysis method.

2. New equivalent relationship between sdof structures with AVS systems and so-called fictitious linear structures

The equivalent principle, which was adopted in paper [19] to establish an equivalent relationship between sdof structures with AVS systems and so-called fictitious linear structures, was that the peak point on the steady-state displacement amplitude–excitation frequency curve of the fictitious linear structure was in good agreement with that of the sdof active-variable-stiffness structure. Because the interstorey shear forces in structures are related to the inertial forces and acceleration responses of structures, a new equivalent principle that the peak point on the steady-state acceleration amplitude–excitation frequency curve of the fictitious linear structure is in good agreement with that of the sdof active-variable-stiffness structure is adopted in this study, and then a new equivalent relationship between sdof structures with AVS systems and so-called fictitious linear structures is established as follows.

Consider an sdof structure equipped with AVS systems. The equation of motion of the controlled structure subjected to a sinusoidal excitation may be expressed as

$$m\ddot{x} + c\dot{x} + kx + \frac{\Delta k}{2}[1 + \mathrm{sign}(x\dot{x})]x = p\sin\Omega t \tag{1}$$

in which m, k and c are the mass, stiffness and damping coefficient of the uncontrolled structure, respectively; x is the displacement of the controlled structure relative to the ground; Δk is the additional stiffness provided by the stand-by bracings in the AVS systems; p and Ω are the amplitude and frequency of the sinusoidal excitation, respectively; and sign(•) represents a symbol function.

Eq. (1) can be rewritten as

$$\ddot{x} + 2\xi\omega\dot{x} + \omega^2 x + \frac{\omega_a^2}{2}[1 + \mathrm{sign}(x\dot{x})]x = \frac{p}{m}\sin\Omega t, \tag{2}$$

where $\omega = \sqrt{k/m}$ and $\xi = c/2m\omega$ are, respectively, the circular frequency and damping ratio of the uncontrolled structure; $\omega_a = \sqrt{\Delta k/m}$ is the additional circular frequency due to the stand-by bracings.

As mentioned above, the following control algorithm proposed by Kobori and Kamagata is adopted in this study:

$$\text{if } x(t)\dot{x}(t) > 0: \text{ the stand-by bracings are locked and } \mathrm{sign}(x\dot{x}) = 1, \tag{3}$$

$$\text{if } x(t)\dot{x}(t) < 0: \text{ the stand-by bracings are unlocked and } \mathrm{sign}(x\dot{x}) = -1. \tag{4}$$

Consider different cases listed in Table 1. The acceleration time histories of the controlled and uncontrolled structures for Case 3 with $\Omega/2\pi = 0.4\,\mathrm{Hz}$ and Case 9 with $\Omega/2\pi = 0.9\,\mathrm{Hz}$ are, respectively, shown in Figs. 1(a) and (b). It is observed from these figures that with an increase in the excitation time, the acceleration response of the controlled structure that involves strong

Table 1
Cases for numerical simulation

Cases	1	2	3	4	5	6	7	8	9	10	11	12
$\Delta k/k = \omega_a^2/\omega^2$	0.3	0.6	1.0	1.5	2.0	3.0	0.3	0.6	1.0	1.5	2.0	3.0
$\omega/2\pi$ (Hz)			0.5						1.0			
p/m						1.0						
ξ						0.05						
	13	14	15	16	17	18	19	20	21	22	23	24
$\Delta k/k = \omega_a^2/\omega^2$	0.3	0.6	1.0	1.5	2.0	3.0	0.3	0.6	1.0	1.5	2.0	3.0
$\omega/2\pi$ (Hz)			2.0						3.0			
p/m						1.0						
ξ						0.05						

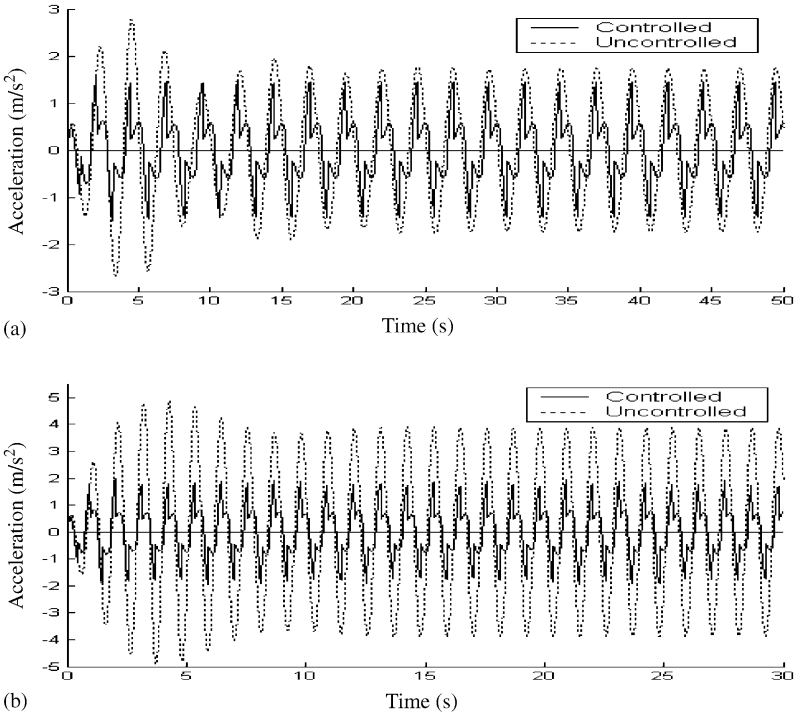

Fig. 1. Acceleration time histories of controlled and uncontrolled structures: (a) Case 3 ($\Omega/2\pi = 0.4$ Hz), (b) Case 9 ($\Omega/2\pi = 0.9$ Hz).

nonlinearity is still in an approximately steady state. Similar results are obtained for other cases and for other frequencies of the sinusoidal excitation. Hence, for each case in Table 1, a steady-state acceleration amplitude–excitation frequency curve can be obtained for the controlled structure.

Referring to the steady-state acceleration amplitude–excitation frequency curve of the controlled structure that is corresponding to a certain case in Table 1, a so-called fictitious linear structure may be constructed as follows:

$$\ddot{x} + 2\xi_f \omega_f \dot{x} + \omega_f^2 x = \frac{p}{m} \sin \Omega t, \tag{5}$$

in which ξ_f and ω_f are, respectively, the damping ratio and circular frequency of the fictitious linear structure, and may be determined according to the new equivalent principle that the peak point on the steady-state acceleration amplitude–excitation frequency curve of the fictitious linear structure is in good agreement with that of the sdof active-variable-stiffness structure. Let

$$\xi_f = \xi + \xi_e \tag{6}$$

and

$$\omega_f = (1 + \eta_e)^{1/2} \omega \quad (\text{i.e., } k_f = (1 + \eta_e)k), \tag{7}$$

in which ξ_e and η_e are referred to herein as the equivalent additional damping ratio and equivalent additional stiffness ratio, respectively, and k_f is the stiffness of the fictitious linear structure.

Values of ξ_e and η_e corresponding to different cases in Table 1 are presented in Table 2. Considering that the value of $\Delta k/k$ is usually around or less than 1.0 in engineering practice, a regression analysis is carried out only on the data in Table 2 that corresponds to the cases with $\Delta k/k = 0.3, 0.6, 1.0$ and 1.5. The resulting expressions are

$$\xi_e = (-0.0012\rho + 0.0001)\omega - 0.0185\rho^2 + 0.0751\rho + 0.0086 \quad (0.5 \leqslant \omega/2\pi \leqslant 3.0), \tag{8}$$

$$\eta_e = (0.0147\rho - 0.0031)\omega + 0.4206\rho + 0.0334 \quad (0.5 \leqslant \omega/2\pi \leqslant 3.0), \tag{9}$$

Table 2
Equivalent additional stiffness ratio η_e and equivalent additional damping ratio ξ_e

Cases	1	2	3	4	5	6	7	8
ω_f (rad/s)	3.38	3.58	3.85	4.10	4.40	4.92	6.80	7.24
η_e	0.16	0.30	0.50	0.70	0.96	1.46	0.17	0.33
ξ_e (%)	2.8	4.5	6.0	7.3	7.9	8.9	2.8	4.4
	9	10	11	12	13	14	15	16
ω_f (rad/s)	7.75	8.40	9.06	10.22	13.62	14.64	15.91	17.49
η_e	0.52	0.79	1.08	1.65	0.17	0.36	0.60	0.94
ξ_e (%)	5.9	7.0	7.6	8.5	2.7	4.2	5.3	6.1
	17	18	19	20	21	22	23	24
ω_f (rad/s)	19.18	21.76	20.58	22.22	24.36	26.64	29.25	34.11
η_e	1.33	2.00	0.19	0.39	0.67	1.00	1.41	2.27
ξ_e (%)	6.3	6.8	2.4	3.6	4.3	4.7	4.7	3.9

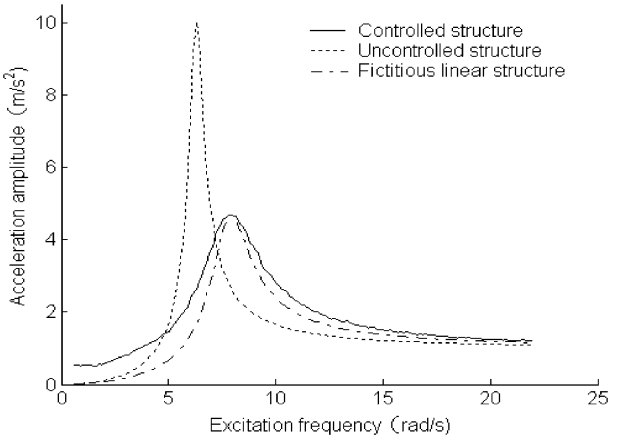

Fig. 2. Comparison of steady-state acceleration amplitude–excitation frequency curve of fictitious linear structure with that of controlled structure for Case 9.

in which $\rho = \Delta k/k = (\omega_a/\omega)^2$ and $0.3 \leqslant \rho \leqslant 1.5$. The maximum errors of ξ_e and η_e obtained from Eqs. (8) and (9) with respect to the corresponding data in Table 2 are 6.65% and 3.99%, respectively.

Fig. 2 shows the steady-state acceleration amplitude–excitation frequency curve of the fictitious linear structure against that of the controlled structure for Case 9 in Table 1. As can be seen, the peak points of the two curves are in good agreement, and the two curves at the right-hand side of the peak points are also close to each other, but the discrepancy between the two curves at the left-hand side of the peak points is significant. Similar results are obtained for other cases in Table 1.

It can be seen from Eqs. (2) and (5) that with a change in the value of and p/m, the acceleration response of the sdof active-variable-stiffness structure and that of the fictitious linear structure vary on a same scale, so the values of ξ_e and η_e determined according to the new equivalent principle are independent of the value of p/m. In this way, although the values of ξ_e and η_e in Table 2, and Eqs. (8) and (9) are obtained under the condition of $p/m = 1$, they are still applicable for other values of p/m.

3. Revised AMS approach for modf structures with AVS systems

The equation of motion for an N-storey building structure equipped with AVS systems in selected storey units and subjected to a horizontal ground acceleration $\ddot{x}_g(t)$ can be written as

$$\mathbf{M}\ddot{\mathbf{X}} + \mathbf{C}\dot{\mathbf{X}} + \mathbf{K}\mathbf{X} + \mathbf{H}\mathbf{U}(t) = -\mathbf{M}\mathbf{I}\ddot{x}_g(t), \tag{10}$$

in which $\mathbf{M}$, $\mathbf{C}$ and $\mathbf{K}$ are the mass, damping and stiffness matrices of the uncontrolled structure, respectively; $\mathbf{X}$ is a column vector with the jth element, x_j, being the displacement of the jth floor relative to the ground; $\mathbf{I}$ is a column vector of "ones"; $\mathbf{H}$ is a constant matrix depending on the locations of the AVS systems; and $\mathbf{U}(t)$ is a control force vector with

the jth element, $u_j(t)$, being

$$u_j(t) = g_j(t)\Delta k_j(x_j - x_{j-1}) \quad (j \geqslant 1), \tag{11}$$

in which $x_0 = 0$ and Δk_j is the additional stiffness provided by the stand-by bracings of the AVS systems installed in the jth storey unit. If there is no AVS system installed in the jth storey unit, then $\Delta k_j = 0$ and $u_j(t) = 0$.

The control algorithm described in Eqs. (3) and (4) may be applied to the N-storey building structure with AVS systems too, but $x(t)$ and $\dot{x}(t)$ shown in these equations should be, respectively, replaced by the interstorey drift and its velocity of the N-storey controlled structure. In this way, $g_j(t)$ in Eq. (11) may be determined as

$$\text{if } (x_j - x_{j-1})(\dot{x}_j - \dot{x}_{j-1}) > 0 \quad (j \geqslant 1):$$

$$\text{Stand-by bracings of the AVS systems installed in the } j\text{th storey are locked, and } g_j(t) = 1, \tag{12}$$

$$\text{if } (x_j - x_{j-1})(\dot{x}_j - \dot{x}_{j-1}) < 0 \quad (j \geqslant 1):$$

$$\text{Stand-by bracings of the AVS systems installed in the } j\text{th storey are unlocked, and } g_j(t) = 0 \tag{13}$$

in which $x_0 = 0$ and $\dot{x}_0 = 0$.

For the uncontrolled structure, the mode-shape matrix $\mathbf{\Phi}$, modal circular frequency vector $\boldsymbol{\omega}$ and modal damping ratio vector $\boldsymbol{\xi}$ are, respectively, expressed as

$$\mathbf{\Phi} = [\boldsymbol{\varphi}_1, \ldots, \boldsymbol{\varphi}_i, \ldots, \boldsymbol{\varphi}_N], \quad \boldsymbol{\omega} = [\omega_1, \ldots, \omega_i, \ldots, \omega_N]^{\mathrm{T}}, \quad \boldsymbol{\xi} = [\xi_1, \ldots, \xi_i, \ldots, \xi_N]^{\mathrm{T}}, \tag{14}$$

in which $\boldsymbol{\varphi}_i$, ω_i and ξ_i are, respectively, the ith mode-shape vector, the ith-mode circular frequency and the ith-mode damping ratio.

For an extreme condition that all the stand-by bracings in the structure are locked, the mass and damping matrices of the controlled structure are, respectively, identical with $\mathbf{M}$ and $\mathbf{C}$ given in Eq. (10), but now the stiffness matrix of the controlled structure has a form of $\mathbf{K} + \Delta\mathbf{K}_{\max}$, in which, $\Delta\mathbf{K}_{\max}$ is the additional stiffness matrix due to all the stand-by bracings in the structure, and has the same form as $\mathbf{K}$ except that k_j (i.e., the stiffness of the jth storey unit of the uncontrolled structure) in $\mathbf{K}$ is replaced by the additional stiffness Δk_j in $\Delta\mathbf{K}_{\max}$. For the extreme condition, the mode-shape matrix and the modal circular frequency vector of the controlled structure are, respectively, written as

$$\mathbf{\Phi}_c = [\boldsymbol{\varphi}_{c1}, \ldots, \boldsymbol{\varphi}_{ci}, \ldots, \boldsymbol{\varphi}_{cN}], \quad \boldsymbol{\omega}_c = [\omega_{c1}, \ldots, \omega_{ci}, \ldots, \omega_{cN}]^{\mathrm{T}}. \tag{15}$$

Suppose the dynamic response of the N-storey building structure with AVS systems may be approximately expressed as

$$\mathbf{X} \approx \sum_{r=1}^{l} q_r(t)\boldsymbol{\varphi}_r \quad (l \leqslant N), \tag{16}$$

in which $q_r(t)$ $(r = 1, 2, \ldots, N)$ is the rth-mode coordinate.

Introducing the expression of $\mathbf{X}$ into Eq. (10), and then premultiplying each term in this equation by $\boldsymbol{\varphi}_i^{\mathrm{T}}$ gives

$$\boldsymbol{\varphi}_i^{\mathrm{T}}\mathbf{M}\sum_{r=1}^{l}\boldsymbol{\varphi}_r\ddot{q}_r(t)+\boldsymbol{\varphi}_i^{\mathrm{T}}\mathbf{C}\sum_{r=1}^{l}\boldsymbol{\varphi}_r\dot{q}_r(t)+\boldsymbol{\varphi}_i^{\mathrm{T}}(\mathbf{K}+\Delta\mathbf{K})\sum_{r=1}^{l}\boldsymbol{\varphi}_r q_r(t)=-\boldsymbol{\varphi}_i^{\mathrm{T}}\mathbf{M}\mathbf{I}\ddot{x}_g(t), \tag{17}$$

in which $\Delta\mathbf{K}$ is the additional stiffness matrix provided by the stand-by bracings in the structure. For the extreme condition mentioned above, we have $\Delta\mathbf{K}=\Delta\mathbf{K}_{\max}$, but for another extreme condition that all the stand-by bracings in the structure are unlocked, $\Delta\mathbf{K}$ is a null matrix. In general conditions, i.e., some stand-by bracings are locked and the others are unlocked, $\Delta\mathbf{K}$ varies from a null matrix to $\Delta\mathbf{K}_{\max}$.

Because the mass and damping matrices of the uncontrolled structure satisfy the orthogonality condition, Eq. (17) may be rewritten as

$$\ddot{q}_i(t)+2\xi_i\omega_i\dot{q}_i(t)+\frac{\boldsymbol{\varphi}_i^{\mathrm{T}}(\mathbf{K}+\Delta\mathbf{K})\sum_{r=1}^{l}\boldsymbol{\varphi}_r q_r(t)}{\boldsymbol{\varphi}_i^{\mathrm{T}}\mathbf{M}\boldsymbol{\varphi}_i}=-\gamma_i\ddot{x}_g(t), \tag{18}$$

in which $\gamma_i=\boldsymbol{\varphi}_i^{\mathrm{T}}\mathbf{M}\mathbf{I}/\boldsymbol{\varphi}_i^{\mathrm{T}}\mathbf{M}\boldsymbol{\varphi}_i$.

Suppose the controlled structure vibrates only in the ith mode. Here, only two states exist for all the stand-by bracings in the structure: locked simultaneously or unlocked simultaneously [20]. When $q_i(t)\dot{q}_i(t)>0$, all the stand-by bracings are locked and $\Delta\mathbf{K}$ is equal to $\Delta\mathbf{K}_{\max}$. In this case, replacing the elements of $\boldsymbol{\Phi}$, in the third term on the left-hand side of Eq. (18), approximately by the corresponding elements of $\boldsymbol{\Phi}_c$ gives

$$\ddot{q}_i(t)+2\xi_i\omega_i\dot{q}_i(t)+\omega_{ci}^2 q_i(t)=-\gamma_i\ddot{x}_g(t). \tag{19}$$

On the other hand, when $q_i(t)\dot{q}_i(t)<0$, all the stand-by bracings are unlocked and $\Delta\mathbf{K}$ is equal to a null matrix. In this case, Eq. (18) may be further written as

$$\ddot{q}_i(t)+2\xi_i\omega_i\dot{q}_i(t)+\omega_i^2 q_i(t)=-\gamma_i\ddot{x}_g(t). \tag{20}$$

Eqs. (19) and (20) may be regarded as two special cases of a sdof active-variable-stiffness system that is

$$\ddot{q}_i(t)+2\xi_i\omega_i\dot{q}_i(t)+\omega_i^2 q_i(t)+\frac{\omega_{ci}^2-\omega_i^2}{2}\left[1+\mathrm{sign}(q_i\dot{q}_i)\right]q_i(t)=-\gamma_i\ddot{x}_g(t). \tag{21}$$

It is observed that the left-hand side of Eq. (21) has a similar form as that of Eq. (2), except that ω_a^2 in Eq. (2) is replaced by $\omega_{ci}^2-\omega_i^2$ in Eq. (21). Hence, referring to the new equivalent relationship between sdof structures with AVS systems and so-called fictitious linear structures discussed in Section 2, the left-hand side of Eq. (21) may be approximately expressed in a form, which is similar to that of Eq. (5), as

$$\ddot{q}_i(t)+2\xi_{fi}\omega_{fi}\dot{q}_i(t)+\omega_{fi}^2 q_i(t)=-\gamma_i\ddot{x}_g(t), \tag{22}$$

in which ξ_{fi} and ω_{fi} may be, respectively, written as $\xi_{fi}=\xi_i+\xi_e$ and $\omega_{fi}=(1+\eta_e)^{1/2}\omega_i$, according to Eqs. (6) and (7), and here ξ_e and η_e are, respectively, determined by Eqs. (8) and (9) with $\omega=\omega_i$ and $\rho=(\omega_{ci}^2-\omega_i^2)/\omega_i^2$.

The ith-mode coordinate $q_i(t)$ may be obtained by solving Eq. (22), and then the dynamic response of the N-storey structure with AVS systems can be approximately determined according to Eq. (16).

4. Approximate analysis method for maximum interstorey shear forces in structures with AVS systems

The maximum interstorey shear force, $V_{j\max}$, of the jth storey unit of the N-storey building structure equipped with AVS systems may be written as

$$V_{j\max} = \max_{0\leqslant t\leqslant t_{\text{total}}} |F_j(t) + F_{j+1}(t) + \cdots + F_N(t)|, \tag{23}$$

in which t_{total} is the duration of the earthquake excitation $\ddot{x}_g(t)$ and $F_j(t)$ is the inertial force of the jth storey unit. According to the revised AMS approach proposed in Section 3, $F_j(t)$ may be expressed as

$$F_j(t) = m_j\left[\sum_{r=1}^{l} \ddot{q}_r(t)\varphi_{rj} + \ddot{x}_g(t)\right], \tag{24}$$

where m_j is the mass of the jth floor and φ_{rj} is the jth element of the rth mode-shape vector $\boldsymbol{\varphi}_r$.

Thirty artificial earthquake excitations, corresponding to different earthquake intensities and different sites, are adopted in this study. The parameters of the 30 artificial earthquake excitations are listed in Table 3. In generating the artificial earthquakes, the acceleration design spectra suggested in the Code for Seismic Design of Buildings in China are first transformed into power spectra, and then the ground acceleration time histories are obtained randomly according to the power spectra [21]. The 5% damped accceleration response spectra related to the generated earthquakes are compared with the target design spectra in Figs. 3(a)–(c). As can be seen, in spite of the scatter of the acceleration response spectra related to the generated earthquakes, they are still in good agreement with the target design spectra on the whole.

Twenty-seven building structures equipped with AVS systems are considered in this study. The basic properties of these example structures are listed in Table 4. The Rayleigh damping matrix is

Table 3
Parameters of artificial earthquakes

Classification of artificial earthquakes	Site	Earthquake intensity	Number of artificial earthquakes	Average peak ground acceleration (gal)	Standard deviation of peak ground acceleration (gal)
Group A	Class II	9	10	123.26	9.97
Group B	Class II	8	10	61.14	6.91
Group C	Class III	7	10	32.97	3.75

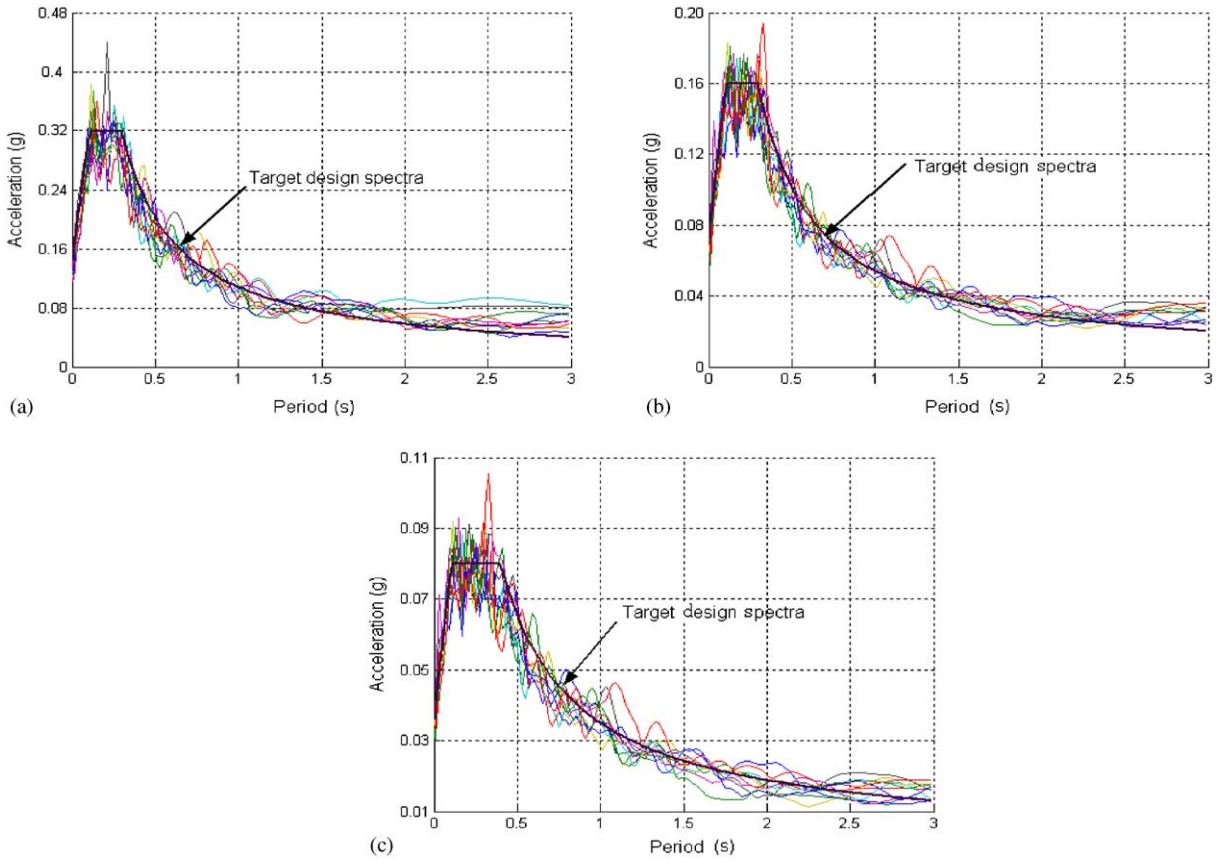

Fig. 3. Comparison of acceleration response spectra related to generated earthquakes with target spectra: (a) Group A, (b) Group B, (c) Group C.

adopted for any of the uncontrolled example structures, and the damping ratio in the first and the second modes is specified by $\xi_1 = \xi_2 = 0.05$.

Extensive numerical simulations, using both the time-history analysis method and the revised AMS approach, are carried out for the 27 building structures equipped with AVS systems and subjected to the 30 artificial earthquake excitations.

Eqs. (8) and (9) are suitable only for the condition of $0.5 \leqslant \omega/2\pi \leqslant 3.0$. So ω_i in Eq. (21) should be restricted to $0.5 \leqslant \omega_i/2\pi \leqslant 3.0$ to make the transformation from Eq. (21) into Eq. (22) feasible. In this way, only the first mode is considered in the numerical simulations, using the revised AMS approach, for structures 1–18, and only the first and the second modes are considered in the numerical simulations, using the revised AMS approach, for structures 19–27.

Denoting β as the ratio of the maximum interstorey shear force obtained using the time-history analysis method to that obtained using the revised AMS approach, the mean value of β, $\bar{\beta}$, for any

Table 4
Basic properties of example structures

Example structure	1	2	3	4	5	6	7	8	9
Total number of storey units N	5	5	5	5	5	5	5	5	5
Mass of each storey m_j (ton) ($j = 1, 2, \ldots, N$)	12.3	12.3	12.3	25.0	25.0	25.0	49.0	49.0	49.0
Stiffness of each storey k_j (10^4 kN/m) ($j = 1, 2, \ldots, N$)	4.87	4.87	4.87	4.87	4.87	4.87	4.87	4.87	4.87
Fundamental period of uncontrolled structure T (s)	0.35	0.35	0.35	0.5	0.5	0.5	0.7	0.7	0.7
$\Delta k_j/k_j$ ($j = 1, 2, \ldots, N$)	0.3	0.6	1.0	0.3	0.6	1.0	0.3	0.6	1.0
	10	11	12	13	14	15	16	17	18
Total number of storey units N	8	8	8	8	8	8	8	8	8
Mass of each storey m_j (ton) ($j = 1, 2, \ldots, N$)	105.6	105.6	105.6	216.0	216.0	216.0	310.5	310.5	310.5
Stiffness of each storey k_j (10^4 kN/m) ($j = 1, 2, \ldots, N$)	25.0	25.0	25.0	25.0	25.0	25.0	25.0	25.0	25.0
Fundamentalperiod of uncontrolled structure T (s)	0.7	0.7	0.7	1.0	1.0	1.0	1.2	1.2	1.2
$\Delta k_j/k_j$ ($j = 1, 2, \ldots, N$)	0.3	0.6	1.0	0.3	0.6	1.0	0.3	0.6	1.0
	19	20	21	22	23	24	25	26	27
Total number of storey units N	12	12	12	12	12	12	12	12	12
Mass of each storey m_j (ton) ($j = 1, 2, \ldots, N$)	175.0	175.0	175.0	275.0	275.0	275.0	396.0	396.0	396.0
Stiffness of each storey k_j (10^4 kN/m) ($j = 1, 2, \ldots, N$)	44.0	44.0	44.0	44.0	44.0	44.0	44.0	44.0	44.0
Fundamental period of uncontrolled structure T (s) 1.0	1.0	1.0	1.25	1.25	1.25	1.5	1.5	1.5	
$\Delta k_j/k_j$ ($j = 1, 2, \ldots, N$)	0.3	0.6	1.0	0.3	0.6	1.0	0.3	0.6	1.0

example structure is defined as

$$\bar{\beta} = \begin{cases} \dfrac{1}{30} \displaystyle\sum_{i=1}^{30} \beta_{iN}, & \text{top floor,} \\ \dfrac{1}{30} \dfrac{1}{N-1} \displaystyle\sum_{i=1}^{30} \sum_{j=1}^{N-1} \beta_{ij}, & \text{other floors,} \end{cases} \tag{25}$$

in which N is the total number of storey units of the example structure and $\beta_{ij} = A_{ij}/B_{ij}$. A_{ij} and B_{ij} are the maximum interstorey shear force of the jth storey unit of the example structure

Table 5
Simulation results of $\bar{\beta}$

Example structure		1	2	3	4	5	6	7	8	9
$\bar{\beta}$	Top floor	1.3905	2.3277	3.9672	1.3457	1.6422	2.1459	1.3080	1.4504	1.6009
	Other floors	1.1718	1.6307	2.6092	1.1153	1.2723	1.5138	1.1050	1.1746	1.3283
		10	11	12	13	14	15	16	17	18
$\bar{\beta}$	Top floor	1.4022	1.9240	3.0735	1.4360	1.6468	2.0509	1.4245	1.5728	1.7452
	Other floors	1.1671	1.3460	1.7131	1.1359	1.2775	1.4858	1.1160	1.2217	1.3878
		19	20	21	22	23	24	25	26	27
$\bar{\beta}$	Top floor	1.2663	1.6967	2.3479	1.2756	1.4876	1.9229	1.2435	1.4265	1.7027
	Other floors	1.1493	1.3268	1.6321	1.1239	1.2773	1.5408	1.0999	1.2173	1.4228

subjected to the ith input artificial earthquake, but A_{ij} is obtained using the time-history analysis method and B_{ij} is obtained using the revised AMS approach. The simulation results of $\bar{\beta}$ for the 27 example structures are given in Table 5 [22].

A regression analysis is carried out on the data in Table 5. The resulting expressions are:

$$\left.\begin{matrix}\Delta k_j/k_j = 0.3 \\ (j = 1, 2, \ldots, N)\end{matrix}\right\} : \bar{\beta} = \begin{cases}(0.0092N - 0.0467)T^{-3} - 0.0199N + 1.4855, & \text{top floor,} \\ (0.0077N - 0.0355)T^{-3} - 0.0010N + 1.1043, & \text{other floors,}\end{cases} \tag{26}$$

$$\left.\begin{matrix}\Delta k_j/k_j = 0.6 \\ (j = 1, 2, \ldots, N)\end{matrix}\right\} : \bar{\beta} = \begin{cases}(0.0524N - 0.2232)T^{-3} - 0.0116N + 1.4560, & \text{top floor,} \\ (0.0155N - 0.0564)T^{-3} + 0.0105N + 1.0775, & \text{other floors,}\end{cases} \tag{27}$$

$$\left.\begin{matrix}\Delta k_j/k_j = 1.0 \\ (j = 1, 2, \ldots, N)\end{matrix}\right\} : \bar{\beta} = \begin{cases}(0.1554N - 0.6671)T^{-3} - 0.0085N + 1.4082, & \text{top floor,} \\ (0.0346N - 0.1118)T^{-3} + 0.0322N + 0.9811, & \text{other floors,}\end{cases} \tag{28}$$

in which T is the fundamental period of the uncontrolled structure and $5 \leqslant N \leqslant 12$.

Based on Eqs. (26)–(28), an approximate analysis method for the maximum interstorey shear forces in structures with AVS systems may be proposed as follows: (a) according to the revised AMS approach presented in Section 3, the maximum interstorey shear force of the jth storey unit, $V_{j\max}$, is primarily estimated by using Eqs. (23) and (24), and (b) to improve the accuracy of the estimated maximum interstorey shear force, a product of $V_{j\max}$ and $\bar{\beta}$ is regarded as the final maximum interstorey shear force of the jth storey unit.

5. Validity of the approximate analysis method for maximum interstorey shear forces in structures with AVS systems

Consider the 27 example structures listed in Table 4 again. The El Centro (NS component), Taft (N21E component) and Kobe (NS component) earthquakes, all scaled to a peak ground

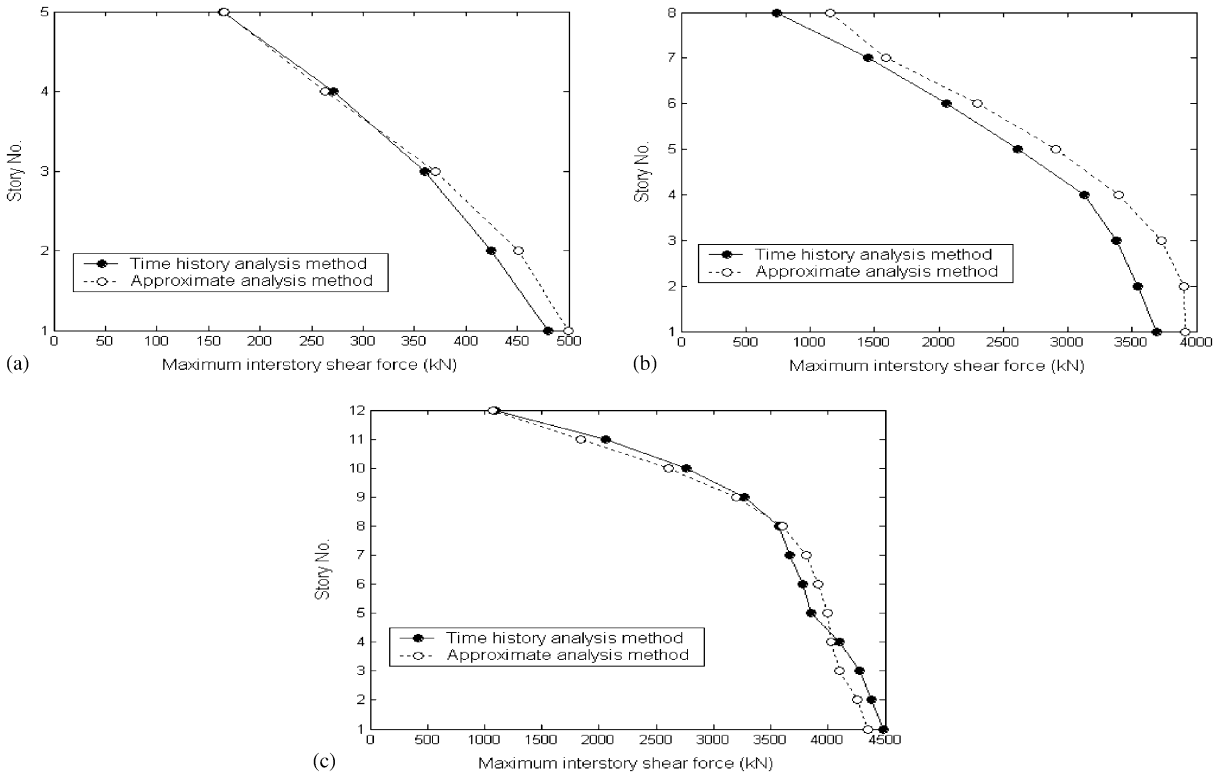

Fig. 4. Maximum interstorey shear forces in example structures under $0.2g$ El Centro earthquake (NS component): (a) example structure 4, (b) example structure 11, (c) example structure 25.

acceleration of $0.2g$, are used as the input excitations. The maximum interstorey shear forces in these example structures subjected to actual earthquake excitations are obtained using the aforementioned approximate analysis method. Some simulation results are shown in Figs. 4–6. For comparison, corresponding results determined using the time-history analysis method are also plotted in these figures.

It is observed from Figs. 4–6 that the maximum interstorey shear forces in example structures obtained using the proposed method generally agree well with those obtained using the time-history analysis method. The errors of the maximum interstorey shear forces obtained using the proposed method with respect to those obtained using the time-history analysis method are mostly less than 10%.

Now consider an 8-storey uncontrolled building structure given by Yang et al. [9]. The mass and stiffness of each storey unit are identical with $m_j = 345.6\,\text{ton}$ and $k_j = 6.8 \times 10^5\,\text{kN/m}$, respectively, for $j = 1, 2, \ldots, 8$. The Rayleigh damping matrix is adopted for the uncontrolled structure, and the damping ratio in the first and the second modes is specified by $\xi_1 = \xi_2 = 0.05$. The AVS systems are installed in every storey units, and the additional stiffness provided by the stand-by bracings of the AVS systems installed in the jth storey unit is $\Delta k_j = 0.6k_j$. The maximum interstorey shear forces in the controlled structure subjected

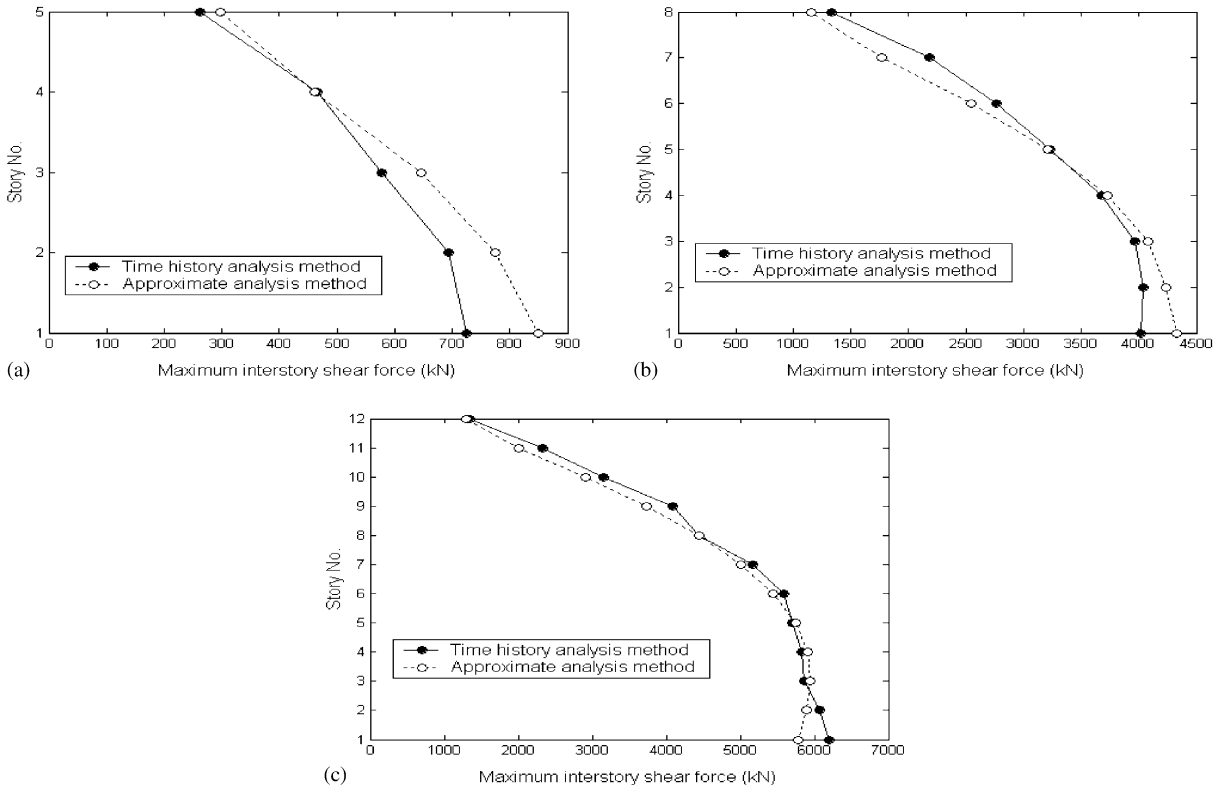

Fig. 5. Maximum interstorey shear forces in example structures under 0.2g Taft earthquake (N21E component): (a) example structure 8, (b) example structure 16, (c) example structure 20.

to the El Centro (NS component), Taft (N21E component) and Kobe (NS component) earthquakes, all scaled to a peak ground acceleration of 0.3g, are obtained using the proposed method. The simulation results are shown in Figs. 7(a)–(c). For comparison, corresponding results determined using the time-history analysis method are also plotted in these figures.

It is observed from Figs. 7(a)–(c) that the proposed method is also effective in estimating the maximum interstorey shear forces in the 8-storey controlled structure subjected to actual earthquake excitations.

In order to check the effect of the locations of AVS systems on the accuracy of the proposed method, Figs. 8(a) and (b) show the maximum interstorey shear forces in the 8-storey building structure with AVS systems located in different selected storey units and subjected to the El Centro earthquake (NS component) with a peak ground acceleration of 0.3g. It can be seen from these figures that the proposed method is still effective in approximately estimating the maximum interstorey shear forces in the 8-storey building structure with AVS systems located in selected storey units, but the estimating precision is a little lower than that shown in Figs. 7(a)–(c).

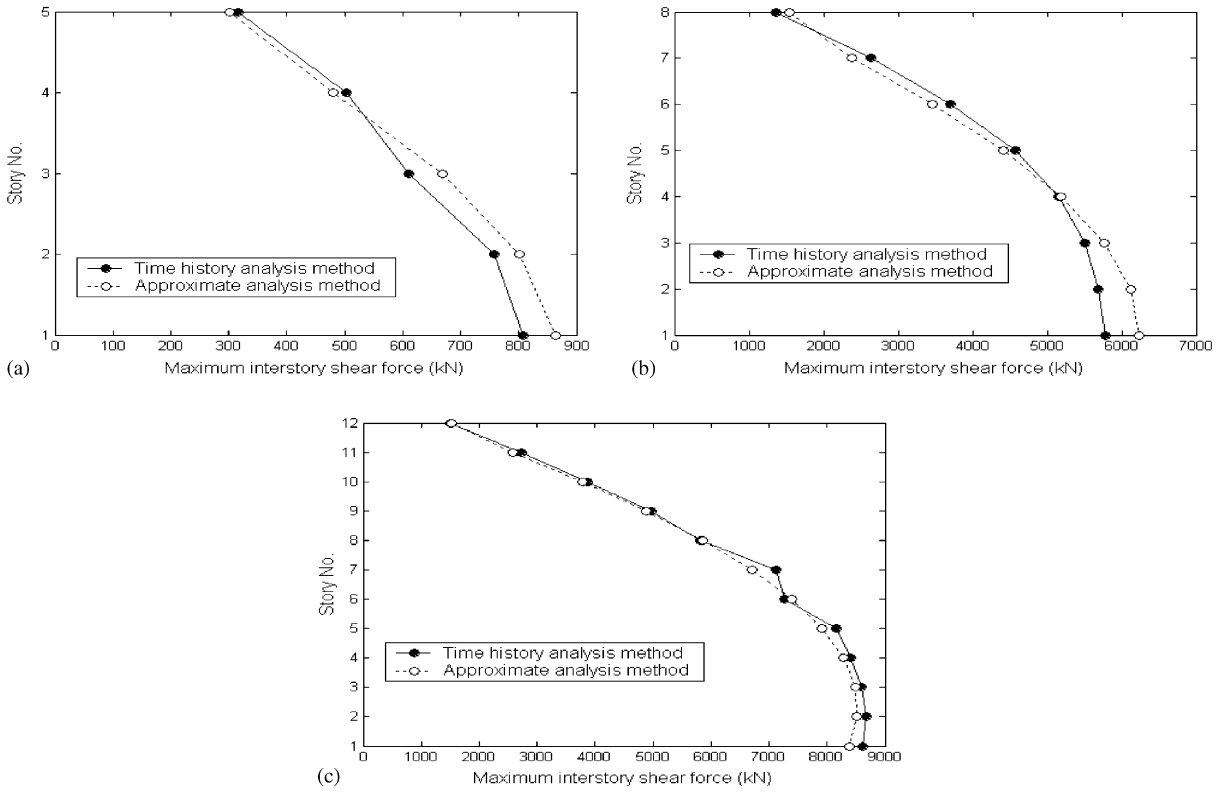

Fig. 6. Maximum interstorey shear forces in example structures under 0.2g Kobe earthquake (NE component): (a) example structure 9, (b) example structure 13, (c) example structure 23.

6. Conclusions

Based on the new equivalent principle that the peak point on the steady-state acceleration amplitude–excitation frequency curve of the so-called fictitious linear structure is in good agreement with that of the sdof active-variable-stiffness structure, a new equivalent relationship between sdof structures with AVS systems and so-called fictitious linear structures is established in this paper. Then, the approximate-mode-superposition (AMS) approach for mdof structures with AVS systems, which was previously suggested by the authors, is revised by using the new equivalent relationship. Subsequently, extensive numerical studies are conducted using the revised AMS approach for the 27 example structures equipped with AVS systems and subjected to the 30 artificial earthquake excitations, and the simulation results are compared with those obtained using the time-history analysis method. Based on the simulation results, an approximate analysis method for the maximum interstorey shear forces in structures with AVS systems is developed. Finally, the accuracy and efficiency of the proposed method are investigated through extensive numerical simulations. The maximum interstorey shear forces in the example structures equipped with AVS systems and subjected to actual earthquake excitations are examined using the proposed method, and the results are compared with those obtained using the time-history

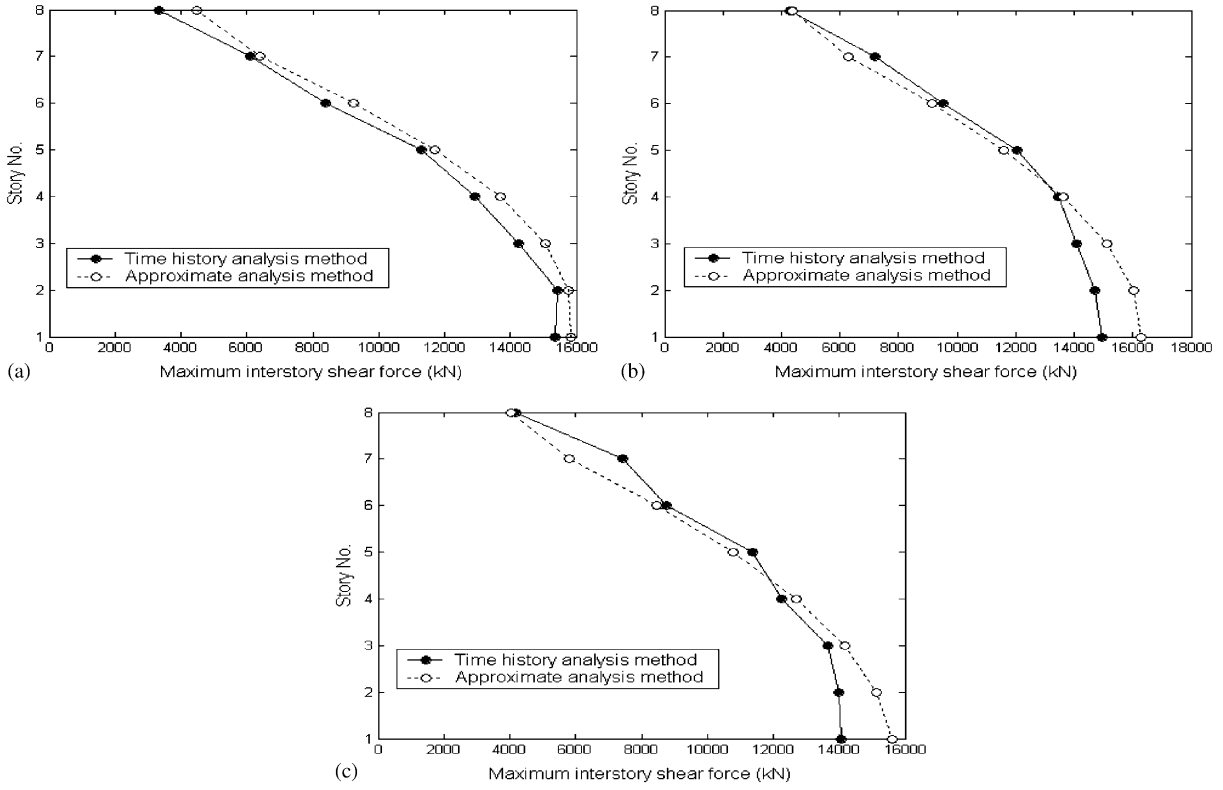

Fig. 7. Maximum interstorey shear forces in the 8-storey structure under 0.3g actual earthquakes: (a) maximum interstorey shear forces in the 8-storey structure under 0.3g El Centro earthquake (NS component), (b) maximum interstorey shear forces in the 8-storey structure under 0.3g Taft earthquake (N21E component), (c) maximum interstorey shear forces in the 8-storey structure under 0.3g Kobe earthquake (NE component).

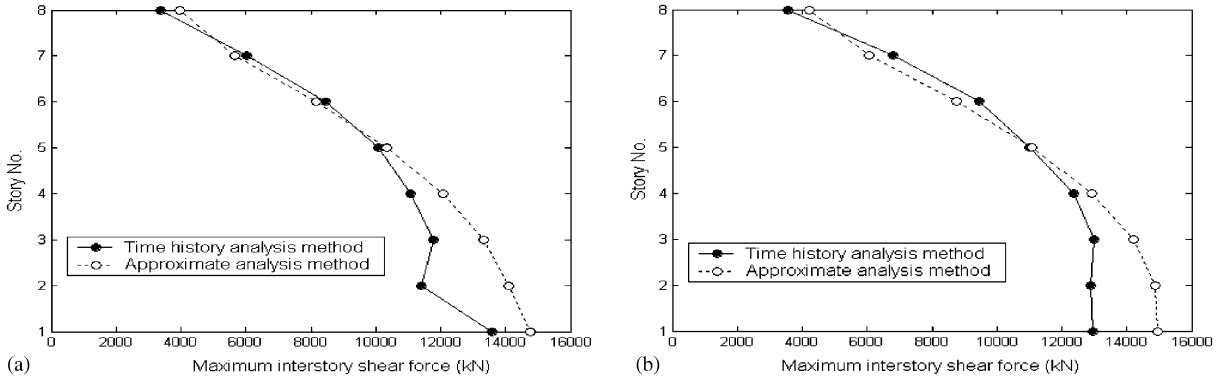

Fig. 8. Maximum interstorey shear forces in the 8-storey structure with AVS systems located in selected storey units and subjected to 0.3g El Centro earthquake (NS component): (a) AVS systems installed in the first, third, fifth and seventh storey units, (b) AVS systems installed in the first, second, third and fourth storey units.

analysis method. It is shown that the maximum interstorey shear forces estimated using the proposed method are generally in good agreement with those obtained using the time-history analysis method. The errors of the maximum interstorey shear forces obtained using the proposed method with respect to those obtained using the time-history analysis method are mostly less than 10% except for several cases. One reason for the errors may be the mutual effect among different modes of the mdof structures, which is not taken into account definitely in the proposed method now. On the other hand, replacing the elements of $\mathbf{\Phi}$, in the third term on the left-hand side of Eq. (18), approximately by the corresponding elements of $\mathbf{\Phi}_c$ perhaps has influence on the errors. Because the proposed method is developed under the condition that AVS systems are installed in every storey units of the 27 example structures, it is mainly fit for building structures with AVS systems added in every storey units. But simulation results indicate that the proposed method is still effective in approximately estimating the maximum interstorey shear forces in structures with AVS systems located in selected storey units; of course the estimating precision is a little lower than that for structures with AVS systems located in every storey units. Currently, efforts are being made to apply the proposed method to the seismic design of building structures with AVS systems.

Acknowledgements

The authors wish to thank the National Natural Science Foundation of China (Project 59895410) for providing the financial support for this investigation.

References

[1] Y. Ikeda, T. Kobori, Active-variable-stiffness system based on instantaneous optimization for single-degree-of-freedom structure, *Journal of Structural and Construction Engineering AIJ* 435 (1992) 51–59.

[2] S. Kamagata, T. Kobori, Autonomous adaptive control of active variable stiffness systems for seismic ground motion, *Proceedings of the first World Conference on Structural Control*, Los Angeles, CA, vol. 2, 1994, TA4-33-TA4-42.

[3] T. Kobori, S. Kamagata, Active variable stiffness system—active seismic response control, in: *Proceedings of the U.S.–Italy–Japan Workshop/Symposium on Structural Control and Intelligent Systems*, Elsevier Science, New York, 1992, pp. 140–153.

[4] T. Kobori, M. Takahashi, T. Nasu, N. Niwa, K. Ogasawara, Seismic response controlled structure with active variable stiffness system, *Earthquake Engineering and Structural Dynamics* 22 (1993) 925–941.

[5] T. Nasu, T. Kobori, M. Takahashi, N. Niwa, K. Ogasawara, Active variable stiffness system with non-resonant control, *Earthquake Engineering and Structural Dynamics* 30 (2001) 1597–1614.

[6] D.C. Nemir, Y. Lin, R.A. Osagueda, Semi-active motion control using variable stiffness, *Structural Engineering* 120 (4) (1994) 1291–1306.

[7] K. Yamada, T. Kobori, Control algorithm for estimating future responses of active variable stiffness structure, *Earthquake Engineering and Structural Dynamics* 24 (1995) 1085–1099.

[8] J.N. Yang, Z. Li, J.C. Wu, Control of seismic-excited buildings using active variable stiffness systems, in: *Proceedings of 1994 American Control Conferences*, IEEE, Piscataway, NJ, 1994, pp. 1083–1088.

[9] J.N. Yang, J.C. Wu, Z. Li, Control of seismic-excited buildings using active variable stiffness systems, *Engineering Structures* 18 (8) (1996) 589–596.

[10] T. Nasu, T. Kobori, M. Takahashi, A. Kunisue, Analytical study on applying the active variable stiffness system to a high-rise building, *Journal of Structural Engineering* 41B (1995) 33–39 (in Japanese).
[11] T. Nasu, T. Kobori, M. Takahashi, A. Kunisue, Analytical study on the active variable stiffness system applied to a high-rise building subjected to the records in Osaka plain during the 1995 Hyogo-ken Nanbu earthquake, *Journal of Structural Engineering* 42B (1996) 1–8 (in Japanese).
[12] T. Nasu, T.Kobori, M. Takahashi, A. Kunisue, Analytical study on a high-rise building with the active variable stiffness system, *Proceedings of the Second World Conference on Structural Control*, vol. 1, 1998, pp. 805–814.
[13] T. Kobori, M. Takahashi, T. Nasu, Experimental study on active variable stiffness system—active seismic response controlled structure, in: *Proceedings of the Fourth World Congress Council on Tall Buildings & Urban Habitat*, 1990, pp. 561–572.
[14] T. Kobori, M. Takahashi, T. Nasu, N. Kurata, J. Hirai, K. Ogasawara, Shaking table experiment of multi-story seismic response controlled structure with active variable stiffness (AVS) system, in: *Proceedings of the Eighth Japan Earthquake Engineering Symposium*, 1990, pp. 1923–1928.
[15] T. Kobori, M. Takahashi, T. Nasu, N. Niwa, N. Kurata, J. Hirai, K. Ogasawara, Shaking table experiment and practical application of active variable stiffness (AVS) system, in: *Proceedings of the Second Conference on Tall Buildings in Seismic Regions, 55th Regional Conference*, 1991, pp. 213–222.
[16] T. Kobori, M. Takahashi, T. Nasu, Dynamic loading test of real scale steel frame with active variable stiffness device, *Journal of Structural Engineering* 37B (1991) 317–328 (in Japanese).
[17] T. Kobori, S. Kamagata, Dynamic intelligent buildings—active seismic response control, in: Y.K. Wen (Ed.), *Intelligent Structures—2: Monitoring and Control*, Elsevier Science, New York, 1992, pp. 279–282.
[18] T. Nasu, T. Kobori, M. Takahashi, Earthquake observation and efficiency evaluation of active variable stiffness system, in: *Proceedings of the Fourth International Conference on Adaptive Structures*, 1993, pp. 15–28.
[19] B. Wu, F.T. Liu, D.M. Wei, Approximate analysis method for displacement responses of structures with active variable stiffness systems, *Earthquake Engineering and Engineering Vibration* 1 (2) (2002) 261–269.
[20] D.P. Feng, Theoretical and Experimental Study on Semi-active Structural Control System, PhD Thesis, Tianjin University, 2000 (in Chinese).
[21] Y.Q. Chen, X.H. Liu, S.L. Gong, Artificial earthquakes compatible with standard response spectrum, *Journal of Building Structures* 2 (4) (1981) 34–43 (in Chinese).
[22] F.T. Liu, Study on Seismic Design Method of Structures with Active Variable Stiffness Systems, Master Thesis, South China University of Technology, 2003 (in Chinese).